LunaPolaris: A stereo camera, point cloud and IMU dataset for future lunar exploration in polar regions

Dave van der Meer[1], Uland Wong[2] and Miguel Olivares-Mendez[1]

***Abstract*— Space missions shift their focus to the lunar surface, for which they require autonomous robots that work in extreme lighting conditions. Most existing datasets used for developing advanced Simultaneous Localisation And Mapping (SLAM) algorithms focus on urban environments like office buildings or cities. Only a limited number of datasets show deserted landscapes without vegetation, and they are usually captured during daylight. Simulations are frequently used in the absence of real or analogue data, but they have fidelity limitations compared to complex planetary environments. The LunaPolaris dataset addresses this issue by providing twelve sequences recorded in a lunar analogue facility using a small rover with a stereo camera, a solid-state LiDAR, and an IMU. These datasets can be used for validating the robustness of visual SLAM or Light Detecting And Ranging (LiDAR)-SLAM in challenging, lunar-like environments, highlighting the challenges around the extreme lighting conditions on the Moon. In this paper, we assess current gaps in existing datasets, present an overview of LunaPolaris, elaborate on the environment and technical details of how the data collection was conducted, and provide initial validation results using stereo and LiDAR SLAM.**

I. Introduction

Recent space missions have shown a high interest in sending rovers to the lunar surface for exploration and resource analysis. These rovers are assembled, developed, and tested on Earth. Given the limited amount of real lunar data suitable for modern robotics needs, the most common methods for system validation are to test the robotic system in either software simulations or inside lunar analogue facilities. Simulations aim to approximate the physical and visual properties of the lunar surface, but their capabilities are often limited by computational resources or in fidelity due to focused research objectives. In many cases, the simulated environments lack the photometric fidelity encountered in real-world applications. A lunar analogue facility replicates the lunar surface environment with high fidelity, while also allowing for hardware-in-the-loop testing of robot engineering models in a physical environment.

The new generation of space rovers places a high emphasis on autonomous automation, enabling continuous operation and improved scalability. The lack of lunar navigation infrastructure requires shipping robots with onboard sensors and performing Simultaneous Localisation And Mapping (SLAM) to obtain trajectory information, and to generate a map of the surroundings of the robot.

Though real lunar data is sparse, the amount of public datasets from lunar analogue facilities is also very limited. This work aims to address this issue by publishing an open-access dataset collected in the LunaLab, a lunar analogue facility at the University of Luxembourg, with a focus on high visual fidelity with respect to the illumination conditions of the Lunar South Pole regions. The data can be found under DOI: 10.5281/zenodo.15737938 on the Zenodo website[1].

The contribution of this work is the generation and publication of an open dataset comprising twelve sequences of lunar analogue terrain and lighting (see Fig. 1). The data is captured using a real robotic platform equipped with a stereo camera, a Light Detecting And Ranging (LiDAR) sensor, and an IMU sensor along with ground truth pose data.

The paper is structured as follows: Section II discusses existing datasets and their limitations for lunar robotics research. Section III presents the lunar analogue facility, the robotic platform, and the data included in the dataset. Section IV highlights efforts to validate the dataset by comparing pose estimations from stereo images and LiDAR data with ground truth. Section V provides examples of dataset applications and recommendations for future work.

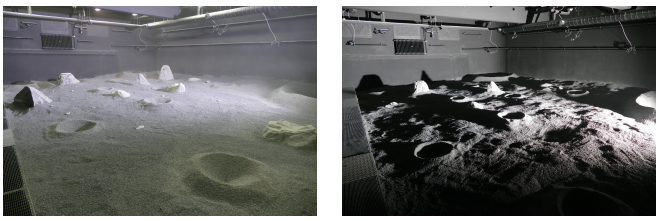

Fig. 1: Two pictures of the LunaLab showing the structure and lighting condition of the environment used for recording the dataset. The left image shows the LunaLab with ambient illumination, with the structural layout of sequence 3. The right shows the LunaLab with the sun simulator light set at the lowest elevation and a few small boulders representing the layout of sequence 5.

II. Related Work

A. Existing datasets

The current state-of-the-art in SLAM methods has a high focus on terrestrial areas, like urban indoor and outdoor

This work was supported by the Luxembourg National Research Fund (FNR) - LUNAR-SLAM project, ref. 17025341.

[1]Affiliated at Space Robotics (SpaceR) Research Group, Interdisciplinary Centre for Security, Reliability and Trust (SnT), University of Luxembourg, Luxembourg, Luxembourg {dave.vandermeer, miguel.olivaresmendez}@uni.lu

[2]Affiliated at NASA Ames Research Center, Mountain View, CA 94035, USA {uland.wong@nasa.gov}

[1]https://zenodo.org/records/15737938

environments or outdoor terrain like forests or fields. There is a multitude of datasets covering these scenarios, such as the KITTI dataset [1], the TUM VI dataset [2] or the HILTI challenge dataset [3]. These datasets often provide terrestrial scenarios in a real-world setup, however they are also considered to be close to ideal-case scenarios with well-lit environments, good weather conditions and rich in visual and geometric features [4]. Other datasets try to address this issue by providing more challenging situations like difficult visual scenes, such as the PennCOSYVIO dataset [5], or scenes with strong visual and geometric degradation through simple corridors, dust, fog, snow, and other weather conditions that cause challenges to SLAM algorithms, such as the SubT-MRS dataset [4].

In the context of space exploration, some datasets are collected in deserted natural environments that represent the surfaces of the Moon or even other planets, such as the Devon Island Rover Navigation dataset [6], the MADMAX dataset [7] or the s3li dataset [8]. Their focus is on real outdoor scenes with partial fidelity to the terrain structure of planetary missions, similar to Mars or the Moon. These datasets typically lack accurate lighting conditions and often contain small amounts of vegetation, which reduces the visual and geometrical fidelity for planetary missions.

To provide a more controlled environment, analogue facilities, such as the lunar test bed at NASA Ames [9], allow for control of the lighting to mimic extreme conditions and replicate the surface structure by using high-fidelity regolith simulants. Additionally, these environments are free from unwanted objects such as vegetation. On the other side, lab environments are sometimes limited by their size, or focus on one aspect of the target environment, and fail to replicate other aspects, such as the consistency of irradiance or the elevation angle of the illumination.

To avoid these physical constraints, while still maintaining full control of the environment, high-fidelity computer simulations, such as the lunar environment simulator OmniLRS [10] or the simulations highlighted in [11], allow for large environments without physical constraints. Simulations come at the cost of visual and geometrical fidelity, as they can mimic the environments only as well as their 3D models are available and of sufficiently high quality.

B. Gaps of existing datasets

The multitude of existing datasets for urban settings are not well-suited for testing algorithms developed for extreme environments with strong visual and structural degradation [1–3]. In contrast, the datasets of the SubT-Challenge [4] do incorporate more extreme conditions, but still do not address planetary surface environments. While the MADMAX [7] dataset is designed for Martian exploration, it is not representative of lunar conditions. Some datasets that focus on lunar-like terrain [6, 8] neglect the illumination conditions of the lunar surface. Additionally, the surface of these lunar-like terrains is covered with coarse rocks, significantly larger than lunar regolith, and the surface does not include any craters, which are present on the Moon. The POLAR Traverse dataset [9] features Lunar-relevant terrain and illumination, but has large movements between images and provides limited variation in motion, mostly representative of straight-line trajectories.

Simulated environments such as in [10, 11] are inherently limited by a sim-to-real gap that cannot be fully resolved through simulation alone.

III. Materials and Methods

The LunaPolaris dataset was collected inside the LunaLab using a small rover equipped with various sensors and by gathering ground truth positioning data. The sequences differ in lighting conditions and geometric landmarks present in the environment.

A. Lunar analogue facility

The LunaLab [12] is a lunar analogue facility with a focus on visual fidelity to represent lunar surface regions such as the lunar South Pole. The facility is equipped with an *Aputure Light Storm 600 C Pro* spotlight with $600\ W$ power output. The spotlight can be adjusted for a colour temperature range from $2,700\ K$ up to $10,000\ K$, and the light intensity can be dimmed. For every sequence, the illumination was set to 100% and the light temperature was set to $5000\ K$. The spotlight can be positioned at its highest position at a distance of $176\ cm$ to the ground and at its lowest position at a distance of $41\ cm$ to the ground. Due to near-field effects, the light height corresponds to an elevation angle between $12.3°$ and $38.7°$ within the testing area for the highest position, and between $2.9°$ and $10.6°$ for the lowest position of the light source, as shown in Fig. 2.

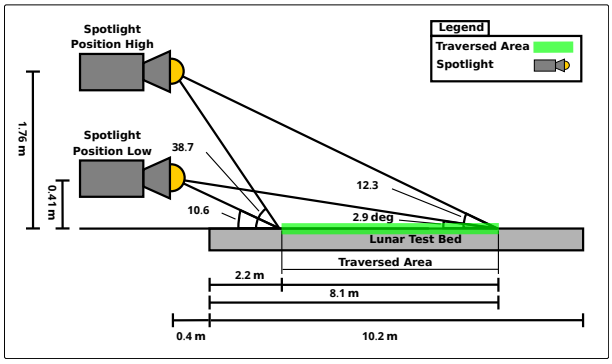

Fig. 2: Visualisation in side view of the elevation angles at different positions inside the LunaLab at different positions of the spotlight

The facility is equipped with a motion capture system and active markers on the robot to capture ground truth pose data with sub-millimetre accuracy. The walls of the facility are painted black to minimise light reflections, resulting in dark and crisp shadows that resemble those on the lunar surface. The ground is covered with basalt of $0.2 - 4\ mm$ in size.

B. Robotic platform

The data for this project is collected using a small mobile robotic platform equipped with a ZED2 stereo camera from

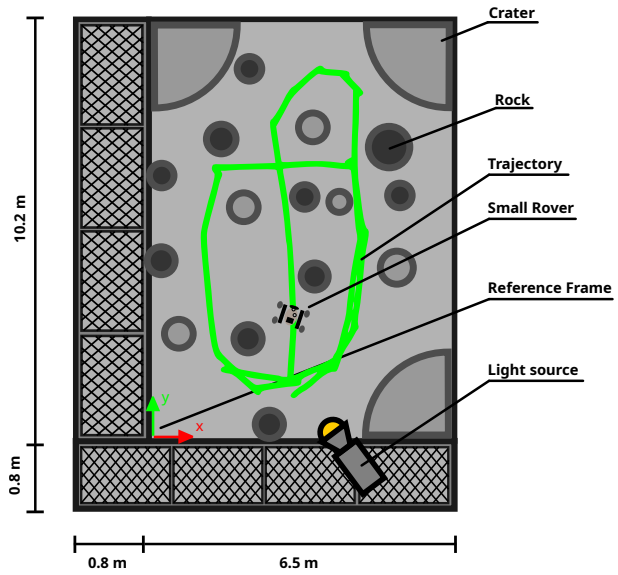

Fig. 3: 2D schematic of the LunaLab including the position of the light, the rocks, the craters, and the robot trajectory

Stereolabs [13], a 3D solid-state LiDAR from Livox [14], and two IMU sensors that are integrated in the camera and LiDAR, as shown in Fig. 4. The footprint of the robot is 40×40 cm and the height is approximately 50 cm to the top part of the robot. The sensor data can be used to perform SLAM for trajectory estimation and sensor fusion. The ground truth data is collected using an active marker from OptiTrack [15] placed on top of the robot. The stereo camera captures 640×360 RGB images at 15 Hz, with a Field of View (FoV) of $110° \times 70°$, and a focal length of 2.12 mm. The camera was set up to use auto-exposure, which ranges from $0.028 - 30$ ms. The ZED2 camera is positioned at the top of the rover, approximately 48 cm above the floor, and tilted downwards by a $25°$ angle. The LiDAR is a solid-state LiDAR with a FoV of $120° \times 25°$, an angular resolution of $0.18° \times 0.23°$, and a scan rate of $452,000$ points per second, publishing at 10 Hz. The LiDAR is positioned below the camera, approximately 33 cm above the floor. The robot uses the Robot Operating System version 2 (ROS 2) Humble and collects data in a rosbag, stored in rosbag files.

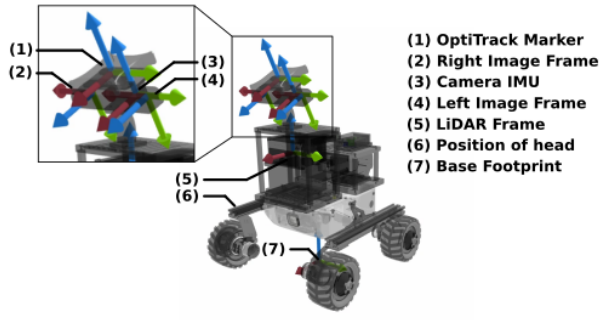

Fig. 4: Small rover with stereo camera, solid state LiDAR, IMU and positioning marker.

C. Data collection

The dataset contains 12 sequences with different illumination conditions and visual and geometrical landmarks. Some images that were recorded contained a glitch where the left and right halves of the images were inverted. These images have been filtered from the final version of the rosbags, and the metadata was updated accordingly. The remaining parts of the data were not touched. Table I shows an overview of these sequences and their respective visual properties. The dataset also contains stereo image pairs for stereo calibration. The images in the dataset use a pinhole camera model with a polynomial distortion model. However, the images are rectified, and hence the distortion coefficients are all zeros. Each sequence traverses the analogue facility using the same trajectory, passing a total of 24 waypoints. At each waypoint, the robot performs a spot turn and then moves forward to the next waypoint. During the forward motion, the robot occasionally stops to correct its heading towards the next waypoint. The maximum linear velocity is set to 0.05 m/s to reduce motion blur, while the maximum rotation speed is 0.1 rad/s. The linear velocity is equivalent to the velocity of the MER rovers [16]. The total trajectory has a length of approximately 30 m. It consists of a complex movement pattern that first circles around the centre of the test bed, then traverses the middle to conclude with a return to the starting position from the opposite direction. Fig. 3 shows the trajectory, starting at the bottom left and first moving towards the right.

The various sequences differ by (1) using three different environmental layouts (see Fig. 5, or by (2) four different lighting conditions. The different layouts contain variable amounts of visual and geometrical landmarks that can be used as reference points for visual or LiDAR SLAM methods. These landmarks mostly consist of small or large boulders distributed on the testing surface. The test bed was designed to have an even distribution of craters and boulders and provide a traversable path for the robot. The trajectory was planned so that the robot has good ground truth acquisition, while avoiding close proximity to the walls of the labs or other structural infrastructure. Additionally, the rover uses a large portion of the available surface and traverses some areas in opposite directions to maximise the total length of the traverse. Some of the boulders were placed such that they hide the infrastructure elements from the view of the robot. The illumination consists of ceiling lights for the first three sequences to have a reference dataset for each layout. For the remaining sequences, a single spotlight is used. For the sequences four to six, the light is positioned at approximately 176 cm from the ground, representing a low elevation angle. For the remaining sequences, a single spotlight at approximately 41 cm from the ground represents a very low elevation angle. The last three sequences feature a second light source mounted in front of the robot, serving as a headlight that illuminates the immediate surroundings of the robot. The trajectory waypoints were kept identical between the sequences to allow for detecting specific conditions

that lead to systematic failures of the odometry estimation. However, the lack of variation in trajectories may introduce a bias towards the testing environment and the viewing angles seen by this specific trajectory.

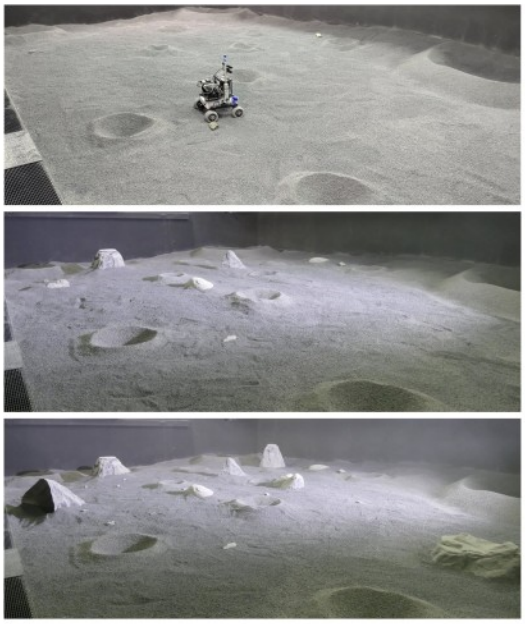

Fig. 5: Pictures of the different layouts of the LunaLab with various amounts of visual and geometrical landmarks.

IV. Evaluation

To evaluate the validity of the dataset, the image data and the LiDAR data were used individually to estimate the trajectory of the robotic platform. The evaluation was done by playing back the rosbags, using ROS 2, as they are published, without further filtering.

The framework for the evaluation of the data in the context of SLAM is called Real-Time Appearance Based Mapping (RTAB-Map) [17]. For Visual Simultaneous Localisation And Mapping (vSLAM), the sequences with lunar lighting conditions were tested using RTAB-Map configured for stereo SLAM; for LiDAR SLAM, the same software was configured to use point cloud data only. For the LiDAR data evaluation, it was assumed that the lighting conditions have an insignificant influence on the LiDAR data. For this reason, only three sequences were used to evaluate the data. However, it was verified that all of the sequences contain the point cloud data.

The results of the trajectory estimations are compared to the ground truth by calculating the Absolute Trajectory Error (ATE) using the EVO tool [18]. Ground truth data are extracted for later comparison with the estimated values.

The feature descriptors are evaluated on a computer running Ubuntu 22.04 with an AMD Ryzen 9 7900X3D 12-Core Processor at 4.7 GHz, 32 GB DDR5 RAM at 5200 MHz, an NVIDIA RTX 4600 TI 16 GB VRAM GPU, 1 TB NVME SSD PCIe Gen4 Storage with a read speed of 7300 MB/s and a write speed of 6600 MB/s.

A. Image data

The image data is evaluated from the rosbags by playing them back while running RTAB-Map using ROS 2. The sequences 4 to 12 were used for applying vSLAM. The first three sequences are recorded with ambient lighting and are points of reference for the performance under indoor illumination. The evaluation limits itself to the sequences using the sunlight simulator for challenging illumination conditions. The ground truth data was extracted from the rosbags and aligned with the time stamps of the estimated poses from RTAB-Map. The results from the EVO tool are used to compare the ground truth with the estimated camera poses.

Table II shows the ATE of the stereo SLAM pose estimates compared to the ground truth poses for the various sequences. Fig. 7a shows the estimated trajectory and the ground truth for sequence 7 using stereo SLAM. The total trajectory of every sequence is approximately 30 meters. It must be noted that the visual odometry failed for sequence 9, and the ATE is shown for the part that was estimated. As a result, the pose estimates had less time to accumulate drift. It should also be noted that the sequences 11 and 12 have extremely high error values after the robot turns towards the light source. This corresponds to an extreme scenario that severely challenges the visual odometry of the robot. These situations require additional research to understand better how to mitigate the negative effects on pose estimation. The odometry loss happened after the camera faced directly into the light source, causing strong visual degradation from lens flares, covering a significant amount of the image, leaving few features from the environment for localisation.

Since the spotlight in sequences 4, 5, and 6 is relatively far from the ground, the elevation angle of the light is relatively high compared to the remaining sequences. This represents a less challenging lighting condition, which is reflected by the rather low ATE.

For sequences 7 to 12, the low angle of incidence of the light caused extreme contrasts between dark shadows and direct illumination of the camera lens, causing major drift among several axes of movement, resulting in higher ATE values.

B. Point cloud data

The point cloud data is evaluated from the rosbags by playing them back while running RTAB-Map using ROS 2. Only the sequences 7, 8, and 9 were used, assuming the influence of the lighting conditions on the point cloud data can be neglected. These three sequences differ in the number of geometric features inside the environment (see Table I).

The ground truth data was extracted from the rosbags and aligned with the time stamps of the estimated poses from RTAB-Map. The results from the EVO tool are summarised in table III. Fig. 7b shows the estimated trajectory and the ground truth for sequence 7 using LiDAR SLAM.

Overall, the pose estimates are rather consistent across the three evaluation scenarios. It is also noticeable that the ATE values are much lower compared to the vSLAM

TABLE I: Sequences arranged by lighting condition and terrain properties.

Lighting Condition	**Craters Only**	**Craters and Small Rocks**	**Craters and Large Rocks**
Ceiling lights	Sequence_01	Sequence_02	Sequence_03
Spotlight High	Sequence_04	Sequence_05	Sequence_06
Spotlight Low	Sequence_07	Sequence_08	Sequence_09
Spotlight Low and Robot Light	Sequence_10	Sequence_11	Sequence_12

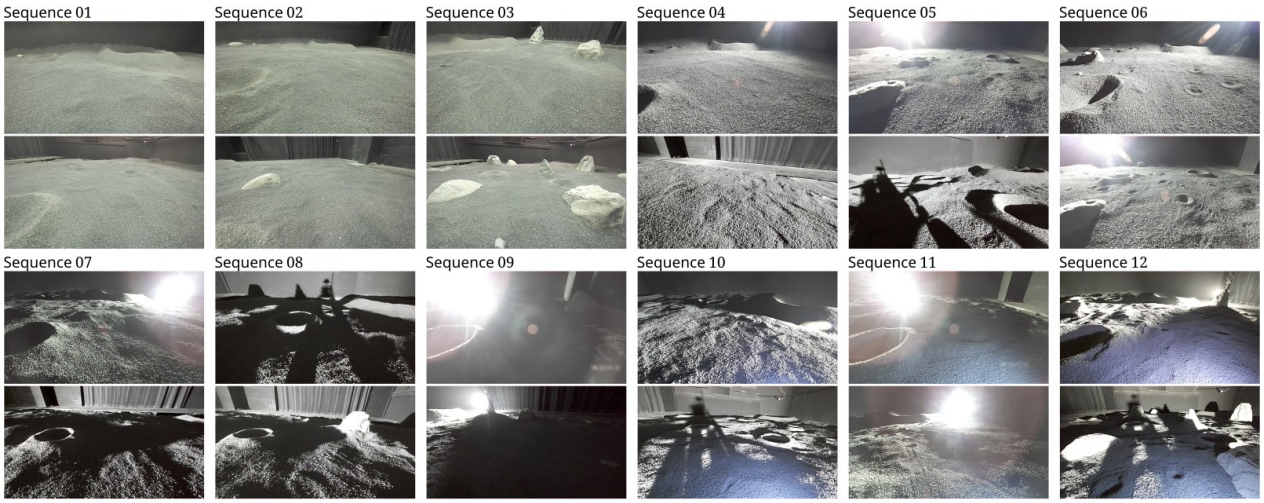

Fig. 6: Overview of image samples from LunaPolaris from all sequences.

TABLE II: ATE values (in metres) for visual SLAM in different lunar lighting conditions.

Sequence	RMSE [m]	Mean [m]	Std [m]	Min [m]	Max [m]	SSE [m^2]
Seq 04	0.25	0.24	0.08	0.07	0.48	9.35
Seq 05	0.11	0.10	0.03	0.02	0.16	1.69
Seq 06	0.32	0.29	0.13	0.05	0.54	17.75
Seq 07	0.12	0.11	0.04	0.01	0.22	2.09
Seq 08	0.23	0.22	0.08	0.05	0.40	8.51
Seq 09	0.11	0.11	0.03	0.06	0.17	0.72
Seq 10	0.09	0.09	0.03	0.02	0.16	1.54
Seq 11	0.44	0.33	0.30	0.06	1.73	35.09
Seq 12	0.51	0.45	0.24	0.08	1.05	43.78

TABLE III: ATE values (in metres) for three different landmark layouts using LiDAR SLAM.

Sequence	RMSE [m]	Mean [m]	Std [m]	Min [m]	Max [m]	SSE [m^2]
Seq 07	0.08	0.08	0.03	0.01	0.17	1.44
Seq 08	0.05	0.05	0.02	0.01	0.13	0.48
Seq 09	0.09	0.09	0.04	0.02	0.19	2.18

experiments. This difference highlights the shortcomings of visual odometry for pose estimation in visually degraded environments. Also, it can be observed that the ATE for sequence 8 is visibly lower compared to sequence 7. This could be explained by the lack of geometrical features in the latter, making it more difficult to align the point clouds at different poses, resulting in lower pose estimation accuracy. Surprisingly, sequence 9 has the highest ATE values, suggesting that more geometrical features do not necessarily increase the accuracy of the pose estimation. Further research is needed to clarify the influence of additional geometric features and their quality for pose estimation.

C. Known Issues

When evaluating the data from the different sequences, a few minor issues were noticed. First, sequence 4 has a moment where the robotic platform stops moving in the second half of the sequence. This was an unplanned stop, most likely due to a temporary failure of the motor driver. A similar stop happened in sequence 6 in the first five minutes of the recording. Second, sequence 7 has a part in the beginning where the frame rate seems higher in the rosbag. This is most likely caused by a bottleneck in recording speed, so that some camera images were dropped from the recording. Third, when reaching the waypoints, the robot stops a little abruptly, causing the camera to shake. This is most likely due to a lack of a PiD controller in the motor driver that would smoothly slow down the robot to a full stop. Fourth, the size of the environment is limited and can not be considered equivalent to an open field. Fifth, the illumination source is close to one edge of the test bed, so the light intensity is not constant across the surface and changes significantly with the inverse-square distance to the light source. Lastly, the size of the basalt on the floor is significantly larger than the regolith on the Moon, due to the high cost of lunar regolith simulant and the safety hazards from small and sharp dust particles in the working environment. Due to the size difference, the images have some noticeable visual differences from images of real regolith.

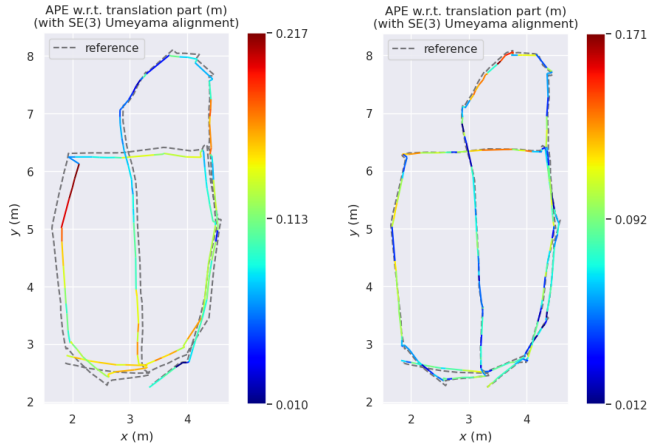

(a) Trajectory estimation of Sequence 07 using stereo SLAM

(b) Trajectory estimation of Sequence 07 using LiDAR SLAM

Fig. 7: ATE of stereo SLAM and LiDAR SLAM applied to sequence 7.

V. Conclusion

This paper presents a new dataset captured with a small robotic platform inside a lunar analogue facility with a focus on high visual fidelity for lunar polar regions. This dataset complements existing planetary visual navigation data by providing continuous sensor readings along a complex trajectory. These properties make it particularly relevant to micro-rover missions, which need to rely on SLAM for autonomous navigation. The dataset includes stereo images, LiDAR sensor data and IMU data and can be used to verify various SLAM approaches for the extreme lunar environment. The evaluation of the image data shows that visual odometry is still lacking the accuracy of LiDAR based SLAM algorithms.

In future work, the image data of this dataset can be used to verify various approaches to increase the accuracy and robustness of vSLAM targeted for use in lunar missions. The LiDAR data can be used for SLAM application to study the influence of different kinds of geometrical features and their quality for pose estimation. The stereo images with the strong visual degradation through the sunlight simulator can be analysed to compare different visual feature detectors and descriptors, and compare them for robustness in lunar environments. These images can also be used to find techniques to mitigate the influence of the lens flares on visual pose estimation and increase the robustness against direct sunlight.

Acknowledgment

This work was supported by the Luxembourg National Research Fund (FNR) - LUNAR-SLAM project, ref. 17025341.

References

[1] A. Geiger, P. Lenz, and R. Urtasun, "Are we ready for autonomous driving? The KITTI vision benchmark suite," in *2012 IEEE Conference on Computer Vision and Pattern Recognition*, ISSN: 1063-6919, Jun. 2012, pp. 3354–3361. DOI: 10.1109/CVPR.2012.6248074. [Online]. Available: https://ieeexplore.ieee.org/document/6248074 (visited on 07/22/2025).

[2] D. Schubert, T. Goll, N. Demmel, V. Usenko, J. Stückler, and D. Cremers, "The TUM VI Benchmark for Evaluating Visual-Inertial Odometry," in *2018 IEEE/RSJ International Conference on Intelligent Robots and Systems (IROS)*, ISSN: 2153-0866, Oct. 2018, pp. 1680–1687. DOI: 10.1109/IROS.2018.8593419. [Online]. Available: https://ieeexplore.ieee.org/document/8593419 (visited on 03/15/2024).

[3] M. Helmberger, K. Morin, B. Berner, N. Kumar, G. Cioffi, and D. Scaramuzza, "The Hilti SLAM Challenge Dataset," *IEEE Robotics and Automation Letters*, vol. 7, no. 3, pp. 7518–7525, Jul. 2022, ISSN: 2377-3766. DOI: 10.1109/LRA.2022.3183759. [Online]. Available: https://ieeexplore.ieee.org/document/9797800 (visited on 07/22/2025).

[4] S. Zhao *et al.*, "SubT-MRS Dataset: Pushing SLAM Towards All-weather Environments," in *2024 IEEE/CVF Conference on Computer Vision and Pattern Recognition (CVPR)*, ISSN: 2575-7075, Jun. 2024, pp. 22 647–22 657. DOI: 10.1109/CVPR52733.2024.02137. [Online]. Available: https://ieeexplore.ieee.org/document/10657540 (visited on 07/10/2025).

[5] B. Pfrommer, N. Sanket, K. Daniilidis, and J. Cleveland, "PennCOSYVIO: A challenging Visual Inertial Odometry benchmark," in *2017 IEEE International Conference on Robotics and Automation (ICRA)*, Singapore, Singapore: IEEE, May 2017, pp. 3847–3854, ISBN: 9781509046331. DOI: 10.1109/ICRA.2017.7989443. [Online]. Available: http://ieeexplore.ieee.org/document/7989443/ (visited on 07/22/2025).

[6] P. Furgale, P. Carle, J. Enright, and T. D. Barfoot, "The Devon Island rover navigation dataset," en, *The International Journal of Robotics Research*, vol. 31, no. 6, pp. 707–713, May 2012, ISSN: 0278-3649, 1741-3176. DOI: 10.1177/0278364911433135. [Online]. Available: https://journals.sagepub.com/doi/10.1177/0278364911433135 (visited on 02/10/2025).

[7] L. Meyer *et al.*, "The MADMAX data set for visual-inertial rover navigation on Mars," en, *Journal of Field Robotics*, vol. 38, no. 6, pp. 833–853, Sep. 2021, ISSN: 1556-4959, 1556-4967. DOI: 10.1002/rob.22016. [Online]. Available: https://onlinelibrary.wiley.com/doi/10.1002/rob.22016 (visited on 07/22/2025).

[8] R. Giubilato, W. Sturzl, A. Wedler, and R. Triebel, "Challenges of SLAM in Extremely Unstructured Environments: The DLR Planetary Stereo, Solid-State LiDAR, Inertial Dataset," *IEEE Robotics and Au-*

tomation Letters, vol. 7, no. 4, pp. 8721–8728, Oct. 2022, ISSN: 2377-3766, 2377-3774. DOI: 10.1109/LRA.2022.3188118. [Online]. Available: https://ieeexplore.ieee.org/document/9813579/ (visited on 07/22/2025).

[9] M. Hansen, U. Wong, and T. Fong, *The POLAR Traverse Dataset: A Dataset of Stereo Camera Images Simulating Traverses across Lunar Polar Terrain under Extreme Lighting Conditions*, arXiv:2403.12194, Mar. 2024. DOI: 10.48550/arXiv.2403.12194. [Online]. Available: http://arxiv.org/abs/2403.12194 (visited on 07/22/2025).

[10] A. Richard *et al.*, *OmniLRS: A Photorealistic Simulator for Lunar Robotics*, arXiv:2309.08997, Sep. 2023. DOI: 10.48550/arXiv.2309.08997. [Online]. Available: http://arxiv.org/abs/2309.08997 (visited on 07/22/2025).

[11] E. Z. Crues *et al.*, "Approaches for Validation of Lighting Environments in Realtime Lunar South Pole Simulations," in *2023 IEEE Aerospace Conference*, ISSN: 1095-323X, Mar. 2023, pp. 1–18. DOI: 10.1109/AERO55745.2023.10115836. [Online]. Available: https://ieeexplore.ieee.org/abstract/document/10115836 (visited on 10/06/2025).

[12] P. Ludivig, A. Calzada-Diaz, M. A. Olivares Mendez, H. Voos, and J. Lamamy, "BUILDING A PIECE OF THE MOON: CONSTRUCTION OF TWO INDOOR LUNAR ANALOGUE ENVIRONMENTS," English, Oct. 2020. [Online]. Available: https://orbilu.uni.lu/handle/10993/45539 (visited on 07/01/2025).

[13] Stereolabs Inc., *Zed 2 stereo camera datasheet*, Accessed: 2025-08-11, 2024. [Online]. Available: https://www.stereolabs.com/datasheets.

[14] Livox Technology Company, *Livox hap high performance lidar sensor user manual*, Accessed: 2025-08-11, 2024. [Online]. Available: https://www.livoxtech.com/hap/specs.

[15] NaturalPoint, Inc., *Optitrack camera specifications and datasheets*, Accessed: 2025-08-11, 2025. [Online]. Available: https://www.optitrack.com.

[16] J. J. Biesiadecki, C. Leger, and M. W. Maimone, "Tradeoffs Between Directed and Autonomous Driving on the Mars Exploration Rovers," en, in *Robotics Research*, S. Thrun, R. Brooks, and H. Durrant-Whyte, Eds., vol. 28, Berlin, Heidelberg: Springer Berlin Heidelberg, 2007, pp. 254–267, ISBN: 9783540481102. DOI: 10.1007/978-3-540-48113-3_23. [Online]. Available: http://link.springer.com/10.1007/978-3-540-48113-3_23 (visited on 10/19/2025).

[17] M. Labbé and F. Michaud, "RTAB-Map as an open-source lidar and visual simultaneous localization and mapping library for large-scale and long-term online operation," en, *Journal of Field Robotics*, vol. 36, no. 2, pp. 416–446, 2019, ISSN: 1556-4967. DOI: 10.1002/rob.21831. [Online]. Available: https://onlinelibrary.wiley.com/doi/abs/10.1002/rob.21831 (visited on 02/16/2022).

[18] M. Grupp, *Evo: Python package for the evaluation of odometry and SLAM.* 2017. [Online]. Available: https://github.com/MichaelGrupp/evo.